Femtosecond Mid-Infrared Study of the Dynamics of Water Molecules in Water–Acetone and Water–Dimethyl Sulfoxide Mixtures

S. Lotze,* C. C. M. Groot, C. Vennehaug, and H. J. Bakker

FOM-Institute for Atomic and Molecular Physics AMOLF, Science Park 104, 1098 XG Amsterdam, The Netherlands

ABSTRACT: We study the vibrational relaxation dynamics and the reorientation dynamics of HDO molecules in binary water–dimethyl sulfoxide (DMSO) and water–acetone mixtures with polarization-resolved femtosecond mid-infrared spectroscopy. For low solute concentrations we observe a slowing down of the reorientation of part of the water molecules that hydrate the hydrophobic methyl groups of DMSO and acetone. For water–DMSO mixtures the fraction of slowed-down water molecules rises much steeper with solute concentration than for water–acetone mixtures, showing that acetone molecules show significant aggregation already at low concentrations. At high solute concentrations, the vibrational and reorientation dynamics of both water–DMSO and water–acetone mixtures show a clear distinction between the dynamics of water molecules donating hydrogen bonds to other water molecules and the dynamics of water donating a hydrogen bond to the S═O/C═O group of the solute. For water–DMSO mixtures both types of water molecules show a very slow reorientation. The water molecules forming hydrogen bonds to the S═O group reorient with a time constant that decreases from 46 ± 14 ps at X_{DMSO} = 0.33 to 13 ± 2 ps at X_{DMSO} = 0.95. The water molecules forming hydrogen bonds to the C═O group of acetone show a much faster reorientation with a time constant that decreases from 6.1 ± 0.2 ps at X_{acet} = 0.3 to 2.96 ± 0.05 ps at X_{acet} = 0.9. The large difference in reorientation time constant of the solute-bound water for DMSO and acetone can be explained from the fact that the hydrogen bond between water and the S═O group of DMSO is much stronger than the hydrogen bond between water and the C═O group of acetone. We attribute the strongly different behavior of water in DMSO-rich and acetone-rich mixtures to their difference in molecular shape.

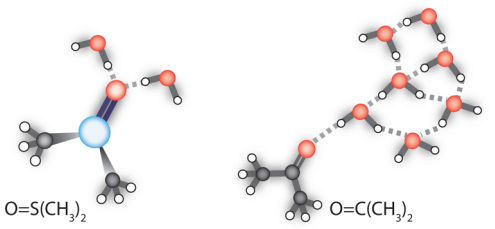

1. INTRODUCTION

Both acetone and DMSO molecules are polar, amphiphilic molecules possessing hydrophobic groups in the form of two methyl groups. Despite their apparent similarity in terms of their molecular formula, acetone and DMSO show large differences in many of their physical properties such as the dipole moment (μ(DMSO) = 3.96 D, μ(acetone) = 2.9 D), the dielectric constant (ϵ(DMSO) = 48, ϵ(acetone) = 21),[1] and the phase transition temperatures (T_{melt}(acetone) = −94.5 °C, T_{melt}(DMSO) = 18.5 °C, T_{boil}(acetone) = 56 °C, T_{boil}(DMSO) = 191.6 °C).[2] These differences likely find their origin in the different structures of DMSO and acetone. The geometry of DMSO differs from that of acetone due to the presence of a lone electron pair on the sulfur atom of DMSO, causing the molecule to adapt a trigonal-bipyramidal shape, which implies that the S═O group is tilted out of the C–S–C plane. For acetone the C═O group is in the C–C–C plane, making the molecule essentially planar.

Aqueous solutions of both compounds have long been known to show highly nonideal behavior, exhibiting a strongly nonlinear behavior with sample composition in various physicochemical properties such as the enthalpy of mixing,[3,4] the viscosity,[5,6] the dielectric relaxation times,[7,8] and the self-diffusion coefficients.[9,10] For example, a water–dimethyl sulfoxide (DMSO) mixture with a molar fraction X_{DMSO} = 0.33 (X_{wat} = 0.67) has a freezing point of −70 °C,[11] whereas pure water and DMSO have freezing points of 0 and 17 °C. This latter property, together with DMSO's ability to permeate the cell wall,[12] has led to its widespread use as a cryoprotective agent in many cell-biological and medical applications.[11,13−16] At the same time, the ability to penetrate the cell wall has also been linked to the neurotoxic effects of DMSO.[17]

The deviation from nonideal behavior indicates that the aqueous mixtures of both compounds are strongly affected by hydrogen-bonding interactions with water molecules. Especially for DMSO–water mixtures, evidence for strong associative interactions has been found, and the nonideal behavior has been explained from the formation of stable DMSO–water complexes with a well-defined stoichiometry of 1:1 or 1:2.[18−20] The exact structure of such complexes is still a matter of debate. Using molecular dynamics simulations, Borin and Skaf[18] observed the prevalence of 1:2 DMSO–water complexes with both water molecules donating a hydrogen bond to the S═O group over a large composition range; only at low water content a stronger tendency for water molecules to bridge two DMSO molecules via hydrogen bonds was found. Neutron diffraction studies of water–DMSO mixtures[21] and simulation work based on molecular dynamics[19,20] came to similar

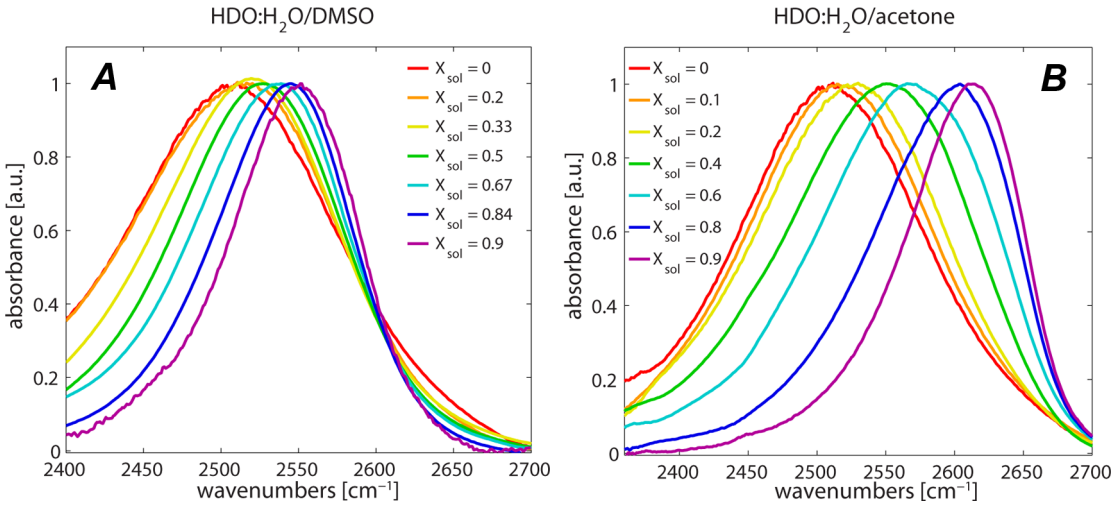

Figure 1. Linear absorption spectra of the OD-stretch region of solutions of (A) DMSO and (B) acetone in 8% HDO:H_2O for various sample compositions. The spectra in panels A and B have been corrected for the solvent background by subtracting the absorption spectrum of either neat H_2O or a solution of H_2O in DMSO or acetone. The latter procedure has been applied to samples with $X_{sol} \geq 0.2$ in order to properly subtract resonances around 2575−2650 cm^{-1} that arise from either acetone or DMSO molecules and the exact resonance frequency of which is sensitive to sample composition and hence to X_{sol}.

conclusions. In contrast, electronic structure calculations by Reiher and co-workers[22] showed that the most stable configuration of 1:2 DMSO−water complexes is formed by a configuration in which the oxygen atom of the S═O group acts as a hydrogen-bond acceptor for only one water molecule, with the second water molecule binding preferentially to this water molecule. In recent work employing two-dimensional infrared and optical Kerr effect spectroscopy, Wong et al. showed that the spectral diffusion dynamics and reorientation of water molecules are significantly affected by the presence of DMSO, and it was suggested that the observed dynamics are linked to the collective reorientation of solute−solvent complexes.[23]

Molecular dynamics simulations and far-infrared absorption experiments have provided evidence that water−acetone mixtures possess a less associative character than water−DMSO mixtures and instead tend to segregate into solute and solvent clusters.[24,25] A comparative neutron scattering and molecular dynamics simulation study of aqueous DMSO and acetone solutions[26] came to similar conclusions, and the differences between binary aqueous DMSO and acetone solutions were explained from differences in the strength of the hydrogen bonds formed between water and the solute molecules. However, other studies found evidence for the presence of an essentially random distribution of water molecules in acetone.[27,28]

Here, we report on a femtosecond infrared study of the hydrogen-bond dynamics in the binary mixtures of water−acetone and water−DMSO over a wide composition range. We study the isotropic and anisotropic vibrational dynamics of water molecules in these mixtures with molar fractions of water X_{wat} ranging from 0.05 to 1, thereby covering both the situation where acetone and DMSO act as a solute in a dilute aqueous solution (high X_{wat}), and the regime of low X_{wat}, where acetone and DMSO act as a solvent and water molecules take the role of the solute.

2. EXPERIMENT

We measure the vibrational relaxation dynamics of the OD stretch vibration of HDO molecules in binary water−acetone and water−DMSO mixtures with molar fractions of solute in the range X_{sol} = 0−0.95. The femtosecond pulses required for this study are generated by a series of nonlinear frequency conversion processes that are pumped with the pulses of a commercial Ti:sapphire regenerative amplifier (Spectra-Physics Hurricane). The amplifier system delivers 100 fs pulses centered around 800 nm with a pulse energy of 0.8 mJ. About 500 μJ of the amplifier output is split off to pump a white-light seeded optical parametric amplifier (OPA, Spectra-Physics) based on β-barium borate (BBO), generating signal and idler pulses with a wavelength around 1333 and 2000 nm, respectively. The idler pulses are frequency-doubled in a second BBO crystal, and the resulting pulses are used as a seed for parametric amplification in a lithium niobate ($LiNbO_3$) crystal pumped by the remaining 300 μJ of 800 nm pulses, leading to the generation of mid-infrared pulses with a wavelength of 3.8−4 μm (2500−2600 cm^{-1}) and a duration of 180 fs. The mid-infrared pulses have a pulse energy of 7−9 μJ and a spectral width of approximately 115 cm^{-1}.

The generated mid-infrared pulses are used in a pump−probe experiment. We generate probe and reference beams by splitting off small portions of the generated mid-infrared pulse with a wedged CaF_2 window. The transmitted light is used as the pump beam. The pump, probe, and reference are focused into the sample by a gold-coated off-axis parabolic mirror (focal length f = 100 mm) and recollimated by an identical mirror. The pump and probe foci are spatially overlapped in the sample. In the experiment we measure the pump-induced transient absorption changes as a function of delay between the pump and the probe pulse. The time delay of the probe is varied with a motorized delay stage. The reference is used for a pulse-to-pulse correction of the intensity fluctuations of the probe beam. The transmitted probe and reference beams are frequency-dispersed with a monochromator (Lot Oriel MSH302), and detected with the two lines of a 2 × 32 mercury−cadmium−telluride (MCT, Infrared associates) array. The pump beam is chopped at a frequency of 500 Hz to detect the pump-induced absorption changes. A variable $\lambda/2$ plate is used to set the polarization of the pump beam at 45° relative to that of the probe light. Behind the sample cell, a rotatable wire-

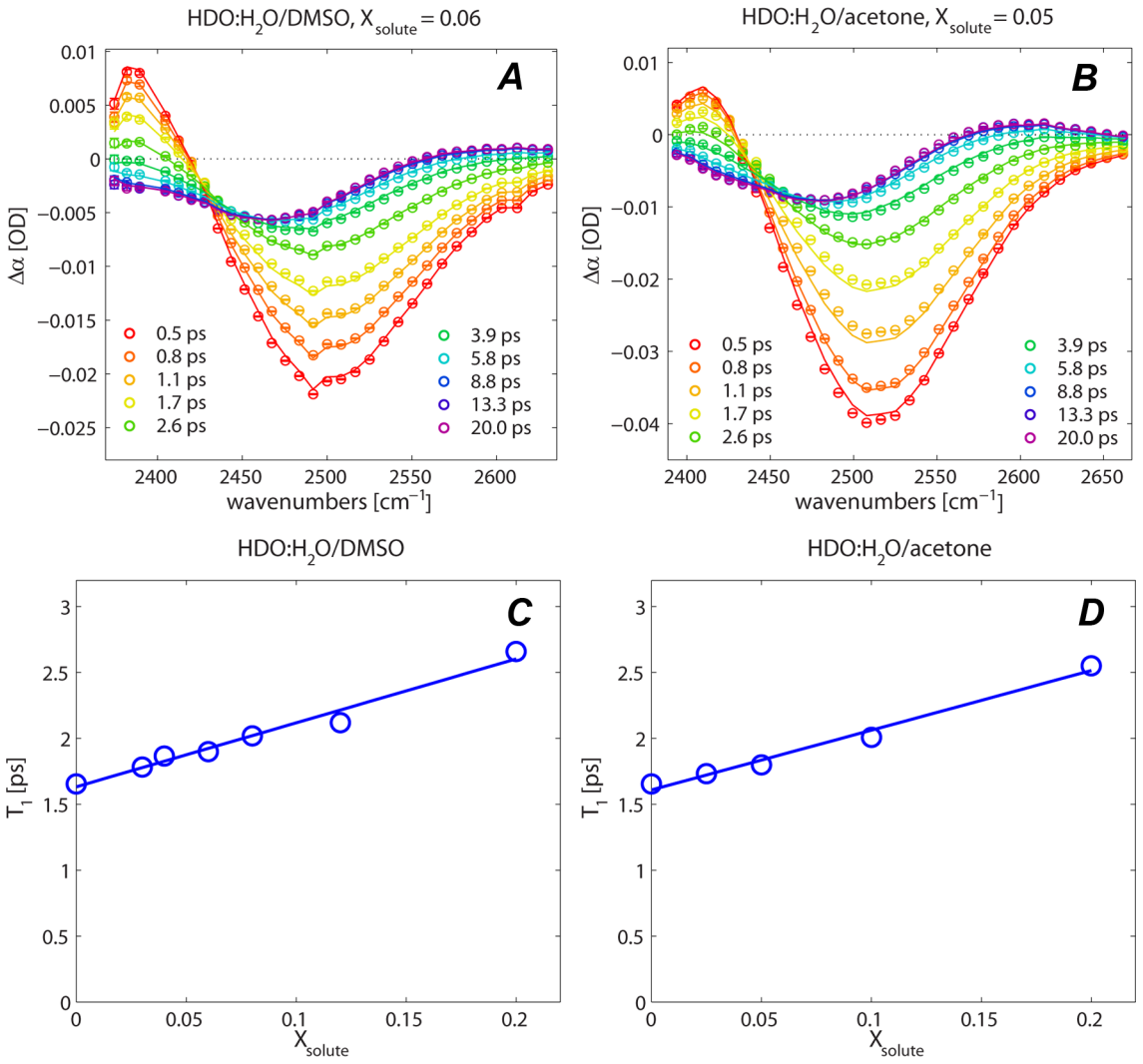

Figure 2. Isotropic transient spectra of (A) water−DMSO solutions with X_{sol} = 0.06 and (B) water−acetone solutions with X_{sol} = 0.05. Open circles are data points, and solid lines are a fit to the model outlined in the text. Panels C and D show the vibrational lifetimes of the OD-stretch vibration (T_1 times) that have been extracted from the fit of the model outlined in the text to the experimental data sets obtained from water−DMSO and water−acetone mixtures, respectively. The solid lines in panels C and D are a guide to the eye.

grid polarizer is placed to select the polarization component of the probe beam parallel or perpendicular to the pump beam. From the parallel ($\Delta\alpha_{\parallel}$) and perpendicular ($\Delta\alpha_{\parallel}$) components of the transient absorption changes, we construct the isotropic signal

$$\Delta\alpha_{iso} = 1/3(\Delta\alpha_{\parallel} + 2\Delta\alpha_{\perp}) \quad (1)$$

and the anisotropic signal

$$R(\omega, t) = \frac{\Delta\alpha_{\parallel}(\omega, t) - \Delta\alpha_{\perp}(\omega, t)}{\Delta\alpha_{\parallel}(\omega, t) + 2\Delta\alpha_{\perp}(\omega, t)} \quad (2)$$

The isotropic signal represents the dynamics of the vibrational relaxation and is unaffected by reorientation. The anisotropy parameter $R(\omega,t)$ is proportional to the second-order orientational correlation function of the transition dipole moment of the OD-stretch vibration $C_{\mu\mu} = \langle P_2(\vec{\mu}(0)\cdot\vec{\mu}(t))\rangle$, where P_2 denotes the second Legendre polynomial, and thus allows to monitor the reorientation dynamics of the HDO molecules.

The samples consisted of aqueous (8% HDO:H_2O) mixtures of acetone or DMSO and were held between two CaF_2 windows separated by Teflon spacers with thicknesses ranging from 50 to 500 μm. Acetone (≥99% purity, HPLC grade) and DMSO (water-free, 99.9% purity) were obtained from Sigma-Aldrich and were used without further purification.

3. RESULTS AND DISCUSSION

3.1. Linear Infrared Spectra. In Figure 1 we show FTIR spectra of the OD-stretch region of solutions of either acetone or DMSO in 8% HDO:H_2O over the whole concentration range studied, i.e., for molar fractions of solute X_{sol} ranging from 0 to 0.9. For both solutes, the width of the OD-stretch absorption band is independent of solute concentration for X_{sol} ≤ 0.2 and has approximately the same value (fwhm ≈ 155 cm^{-1}) as for neat HDO:H_2O. This observation indicates that the dissolution of modest quantities of acetone or DMSO does not lead to a severe disruption of the hydrogen-bond network of water. Increasing the molar fraction of the solute causes a pronounced blue-shift of the OD-stretch absorption band, which is generally attributed to a weakening of the hydrogen-bond strength of water. The blue-shift is accompanied by a reduction in line width down to approximately 85 and 95 cm^{-1}

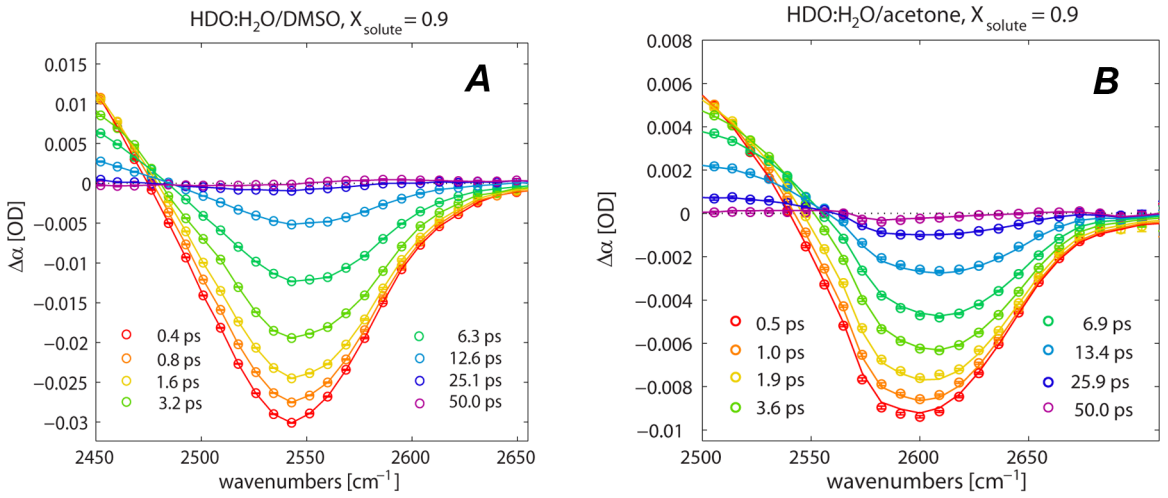

Figure 3. Isotropic transient spectra of (A) water−DMSO solutions with X_{sol} = 0.9 and (B) water−acetone solutions with X_{sol} = 0.9. The open circles represent the data points, and the solid lines are a fit to the model described in the text.

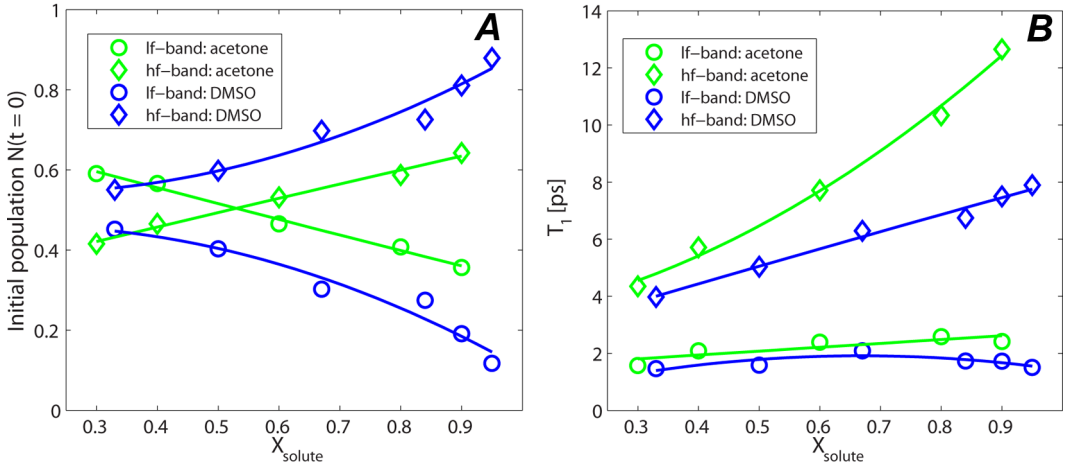

Figure 4. Fit results obtained from the isotropic transient absorption data of water−acetone and water−DMSO solutions with X_{sol} = 0.3−0.95. (A) Integrated spectral amplitude of the bleaching signal of the two components used in the fit of the isotropic transient absorption changes $\Delta\alpha_{iso}(\omega,t)$. (B) Vibrational relaxation times obtained from the fit. Solid lines are a guide to the eye.

full width at half-maximum at X_{sol} = 0.9 for water−DMSO and water−acetone, respectively, suggesting that the distribution of hydrogen-bond strengths in the mixtures becomes substantially less inhomogeneous with increasing solute fraction. For HDO molecules in water−acetone, the OD-stretch absorption band becomes increasingly asymmetric with increasing acetone content, whereas for water−DMSO solutions the band retains a Gaussian shape at all compositions.

3.2. Nonlinear Infrared Spectra and Vibrational Relaxation Dynamics. Figure 2 shows transient absorption spectra of the OD-stretch vibration of HDO molecules in aqueous DMSO (X_{sol} = 0.06) and acetone (X_{sol} = 0.05) solutions for delay times ranging from 0.5 to 20 ps. The linear spectra of these solutions are quite similar to the linear spectrum of pure HDO:H_2O. The transient spectra show a negative response that peaks around 2500−2510 cm^{-1}, originating from the bleaching of the ground state (ν = 0) and stimulated emission from the first excited state (ν = 1) of the oscillator. The positive feature in the transient spectrum observed on the red side of the spectra originates from excited state absorption (ν = 1 → 2). The spectra at late delay times have the shape of a temperature-difference spectrum and result from the thermalization of the vibrational excitation and the energy redistribution over low-frequency degrees of freedom. We find that the data can be well described by a model in which the excited state of the OD-stretch vibration relaxes via an intermediate state to the heated ground state. The intermediate state is included in this model to account for the delayed rise of the thermal signal with respect to the decay of excited state of the OD-stretch vibration. We assume that the intermediate state has the same absorption spectrum as the ground state, meaning that its associated (differential) transient absorption spectrum equals zero at all frequencies. Relaxation from the intermediate state to the ground state likely represents the adaptation of the hydrogen-bonding network to the dissipation of the energy of the vibrational excitation. This model has been successful in describing the vibrational relaxation dynamics of the OD-stretch band in neat HDO:H_2O[29,30] and has also been successfully applied to describe the relaxation of the same mode in aqueous solutions of small amphiphilic solutes.[31]

The results of the fits are shown in Figure 2c,d. This figure shows the vibrational relaxation time (T_1) of the OD-stretch vibration of HDO molecules in water−acetone and water−DMSO mixtures as a function of X_{sol}. We observe that with

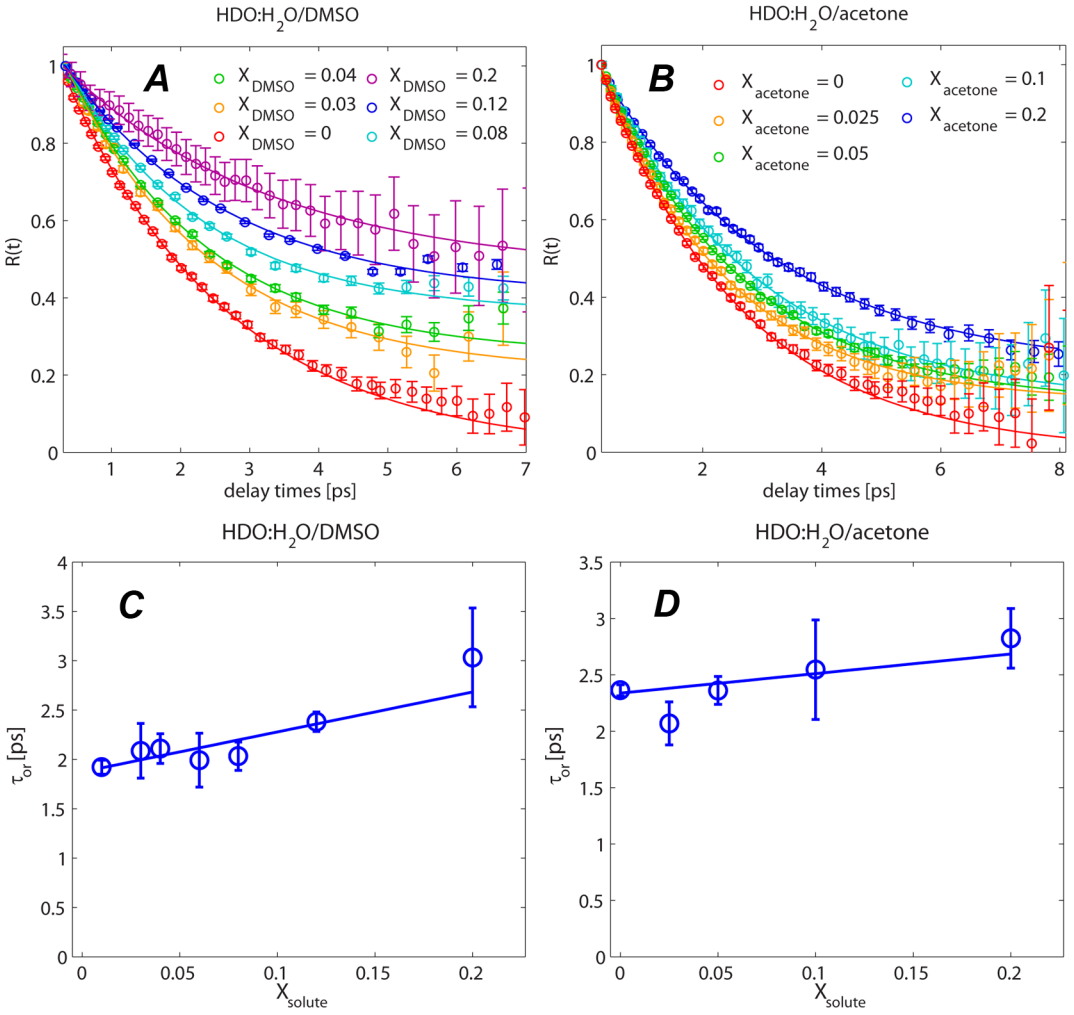

Figure 5. Anisotropy decay of the OD-stretch vibration of HDO molecules in (A) water−DMSO and (B) water−acetone mixtures. The data represent an average over 40 cm^{-1} around the center frequency of the bleach. Open circles represent experimental data points that have been corrected for the time-dependent rise of the thermal end level; solid lines are fits to a function of the form $R(t) = R_1 \exp(-t/\tau_{or}) + R_0$. The reorientation time constants τ_{or} obtained from the fits of the data in panels A and B are plotted in panels C and D, respectively. The solid lines in panels C and D are a guide to the eye.

increasing concentration of either solute the vibrational lifetime increases from 1.65 ps (X_{sol} = 0) to 2.66 ps at X_{sol} = 0.22 (water−DMSO) and to 2.55 ps at X_{sol} = 0.2 (water−acetone), respectively. The gradual increase in T_1 with increasing concentration of solute agrees with the results of previous studies of aqueous solutions of other amphiphilic molecules of comparable size, such as tetramethylurea, proline, and *N*-methylacetamide.[32] The vibrational lifetimes of Figure 2d also agree well with the lifetimes recently reported by Wong et al.[23]

f3 In Figure 3 we show isotropic transient absorption changes of the OD-stretch vibration of HDO molecules with DMSO and acetone in large excess (X_{sol} = 0.9). The maximum of the bleaching signal is clearly shifted to higher frequencies, when compared to the transient spectra in Figure 2. The shifts in the transient spectra of 100 cm^{-1} in the case of water−acetone (Figure 3a) and 50 cm^{-1} in the case of water−DMSO (Figure 3b) are consistent with the blue-shifts of the OD-stretch absorption band in the linear spectra shown in Figure 1a,b. The transient spectra in Figure 3 show a pronounced slowing down of the vibrational relaxation of the OD-stretch vibration compared to Figure 2a,b. The transient spectra Figure 3 also show a blue-shift with increasing delay time, suggesting the presence of subensembles of HDO molecules exhibiting different vibrational lifetimes. In order to account for the presence of different water species, we fit the data of Figure 3a,b with a model that includes two excited states that relax to a common, heated ground state. We employ this model in the analysis of all water−acetone and water−DMSO data sets with X_{sol} > 0.2. The initial populations of the two excited states are allowed to vary in the minimization routine, while the spectral amplitudes are constrained to be equal. This description provides an excellent description of the transient spectral data at all delay times, which shows that the inhomogeneity of the absorption band persists within the experimental time window of ∼10 ps. Hence, there is no rapid exchange between the water species that are associated with the two excited states.

f4 In Figure 4a,b the initial populations and vibrational lifetimes of the two excited states are plotted as a function of X_{sol} for water−acetone and water−DMSO solutions. The increase of the relative amplitude of the high-frequency bands with increasing solute content, as seen in Figure 4a, strongly suggests that the high-frequency bands represent HDO molecules forming hydrogen bonds to the solute. Indeed in previous neutron scattering and molecular dynamics simulation

studies a strong tendency for water molecules to bind to the S═O groups of DMSO was found.[18,21] Likewise, we assign the high-frequency band of OD oscillators in water−acetone mixtures to water molecules forming hydrogen bonds to the C═O groups. For both water−DMSO and water−acetone the vibrational relaxation time constant of the lower frequency band varies in the range 1.5−2 ps (Figure 4b) and is thus comparable to the relaxation rate of the OD-stretch vibration of neat HDO:H_2O. We therefore assign this band to HDO molecules having their OD groups hydrogen bonded to the oxygen atom of other water molecules. The relaxation time constants associated with the high-frequency bands are significantly longer and increase monotonically from approximately 4 ps around X_{sol} = 0.3 to 7.9 ps at X_{sol} = 0.95 for water−DMSO solutions and to 13 ps at X_{sol} = 0.9 for water−acetone solutions. The relatively high frequency and slow relaxation dynamics of these bands indicate that the hydrogen bonds between water and the solute are relatively weak. The more pronounced slowing down of the vibrational relaxation together with the stronger blue-shift of C═O bound waters compared to S═O bound waters in Figures 1 and 3 indicate that water molecules hydrating the C═O groups of acetone form much weaker hydrogen bonds than water molecules hydrating the S═O group of DMSO. This observation is in agreement with the results obtained from calorimetric studies, where an excess enthalpy of mixing of about −2.5 kJ/mol for water−DMSO solutions at X_{DMSO} = 0.33 was reported.[3] Water−acetone mixtures were found to exhibit a maximum negative excess enthalpy of mixing of only −0.67 kJ/mol at X_{acet} = 0.15.[33]

The relative amplitude of the high-frequency band is consistently lower for water−acetone than for water−DMSO solutions. For water−acetone solutions, the amplitude of the low-frequency band, representing HDO molecules bound to other water molecules, is quite large even at X_{sol} = 0.9 (X_{wat} = 0.1). For the water−DMSO solution this amplitude strongly decreases with increasing solute concentration and is only 0.1 at X_{sol} = 0.9. This finding agrees with the linear absorption spectra in Figure 1, where it is seen that the OD-stretch band of water−acetone has a noticeably asymmetric line shape at X_{sol} = 0.9, exhibiting a shoulder on the low-frequency side around ∼2550 cm^{-1}, while the OD-stretch vibration in water−DMSO shows a nearly symmetric, Gaussian line shape.

The large differences between the amplitudes of the spectral bands of the water−acetone and water−DMSO solutions in the range of X_{sol} = 0.3−0.95 can be explained from the different mesoscopic structures of the solutions. Our results suggest that in water−acetone solutions water clusters already form at low X_{wat}, leading to a higher fraction of water molecules hydrogen bonded to other water molecules and a correspondingly lower fraction of water molecules that are hydrogen bonded to C═O. For water−DMSO solutions, the amplitudes of the water-bound and S═O bound water molecules show a concentration dependence that is to be expected in the case of homogeneous mixing, meaning that this system will be far less (microscopically) segregated.

For both water−DMSO and for water−acetone we find that the vibrational relaxation of the OD stretch vibration strongly slows down with increasing solute fraction X_{sol}. This slowing down of the vibrational relaxation can partly be explained from the increased fraction of water molecules that are hydrogen bonded to the S═O and C═O groups. These hydrogen bonds are weaker than the ones between water molecules, which implies that the anharmonic coupling between the OD stretch vibration and the hydrogen bond will be weaker. In addition, with increasing solute fraction it becomes more likely that both hydroxyl groups of these water molecules are bonded to S═O or C═O groups, and it becomes less likely that these water molecules accept hydrogen bonds from other water molecules. Molecular dynamics simulations of water−acetone mixtures[24] and water−DMSO mixtures[18,19] showed that the number of accepted hydrogen bonds per water molecule decreases with increasing solute fraction. The reduced probability of water−water hydrogen bonds is expected to lead to a decrease in the density of accepting modes of the excited hydroxyl stretch vibration, thus causing a decrease in the relaxation rate of water molecules that are hydrogen bonded to C═O or S═O groups, as seen in Figure 4b. This scenario is similar to the one recently proposed by Wong et al. in their study on the vibrational dynamics of water−DMSO solutions.[23]

3.3. Water Reorientation Dynamics at Low Solute Fractions. In Figure 5a,b the anisotropy decay of the OD-stretch vibration of HDO molecules is presented for the composition range X_{sol} = 0.0−0.2. The data have been corrected for the rise of the thermal end level, where we assumed the final heated state to be isotropic. The addition of DMSO or acetone leads to the appearance of a slow component in the decay of the anisotropy, which shows very little decay on a time scale of 8 ps. The amplitude of this component scales with the concentration of solute. This slow component is reminiscent of the slow reorientation component that has been observed in the anisotropy decay of water molecules in the vicinity of hydrophobic groups.[31,32] Therefore, we assign the slow component of Figure 5a,b to water molecules hydrating the hydrophobic methyl groups of DMSO and acetone. The anisotropy curves can be well described by a function of the form $R(t) = R_1 \exp(-t/\tau_{or}) + R_0$. In Figure 5c,d we plot the reorientation time constants that we obtain by fitting this function to the data in Figure 5a,b. For both DMSO and acetone, the values of τ_{or} are very similar to the reorientation time constant of 2−2.5 ps of the OD-stretch vibration in neat HDO:H_2O.[29,30] This finding indicates that the reorientation dynamics are bimodal: a fraction of the water molecules are strongly slowed down in their reorientation by the presence of the solute, whereas the other water molecules are essentially unaffected and exhibit reorientation dynamics comparable to that of water molecules in neat liquid water.

In Figure 6, we plot the ratio of the amplitude of the slow water fraction and the total amplitude of the anisotropy, $R_0/(R_0 + R_1)$, as a function of X_{sol}. These amplitudes have been obtained from fitting the anisotropy curves in Figure 5. We find that the amplitude of the slow water fraction of aqueous DMSO solutions is consistently larger than the amplitude of the slow water fraction in aqueous acetone solutions of the same X_{sol}. This result is surprising, since both solute molecules possess two hydrophobic methyl groups. In a previous femtosecond infrared study, in which the orientational dynamics of water around amphiphilic molecules with different numbers of hydrophobic groups over a similar concentration range as in Figure 6 was studied, the fraction of slowed down water molecules was found to scale linearly with the number of solute methyl groups.[31] The data in Figure 6 suggest that in aqueous acetone solutions fewer water molecules are exposed to the hydrophobic methyl groups than in DMSO solutions. This result indicates that acetone molecules tend to aggregate already at low solute concentrations, thereby reducing the number of methyl groups interacting with water. This

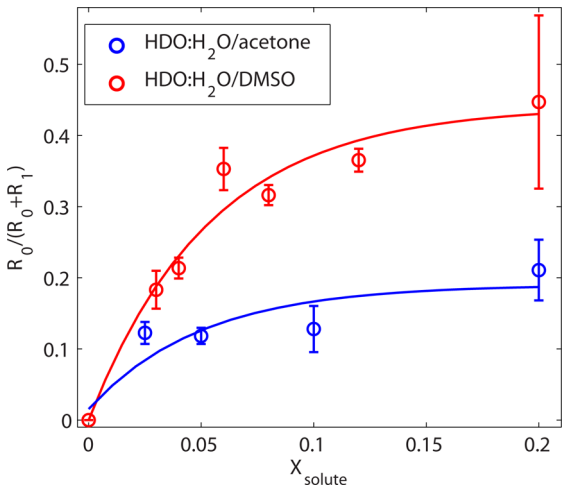

Figure 6. Normalized amplitude of the slow water fractions obtained from the anisotropy decays of Figure 5a,b as a function of X_{sol} for binary mixtures of water and DMSO (red open circles) as well as water and acetone (blue open circles). Solid lines are a guide to the eye.

interpretation agrees well with results from neutron scattering studies of an acetone−water mixture with X_{acet} = 0.05[26] and with results from molecular dynamics simulations.[25]

3.4. Water Reorientation Dynamics at High Solute Fractions.

In Figure 7, we plot the decay of the anisotropy of the OD-stretch vibration of HDO molecules in aqueous DMSO and acetone solutions for a broad composition range 0.1 ≤ X_{sol} ≤ 0.9. The data have been obtained by averaging over a spectral range of 70−100 cm^{-1} of the bleaching signal of the parallel and perpendicular transient absorption spectra. For DMSO we observe the slowest anisotropy decay in the range of X_{DMSO} = 0.33−0.5. This finding agrees with the results of several previous studies that suggested that water and DMSO molecules can form very stable clusters in this composition range. It thus appears likely that the maximum slowdown of water molecules at X_{DMSO} = 0.33−0.5 finds its origin in the formation of stable 1:2 DMSO−water clusters. A further increase of the DMSO concentration is observed to result in a moderate acceleration of the anisotropy decay. It is also seen that the anisotropy decay becomes more single exponential, i.e., less bimodal. It followed from the isotropic data (Figure 4a) that for large X_{DMSO} values the signals are dominated by the response of HDO molecules bound to the S═O groups of DMSO. Hence, in the range of X_{DMSO} = 0.33−0.8, the anisotropy curves of Figure 7a represent a gradual transition from the regime of hydrophobic hydration to a regime where the hydrogen-bonding interaction with the S═O moiety of DMSO starts to determine the anisotropy dynamics. The solute fraction at which we observe the maximum slowdown of water molecules in water−DMSO solutions (X_{DMSO} = 0.33) matches very well with the composition at which theoretical and experimental self-diffusion coefficients show a minimum[9,18] and the composition at which the viscosities[5] and the dielectric relaxation times[7] show a maximum. The observation of a maximum slowing down in dynamics at a particular composition agrees with the results obtained for the spectral diffusion and reorientation dynamics of water molecules in water−DMSO mixtures reported by Wong et al.[23]

For water−acetone mixtures (Figure 7b) the anisotropy decay is observed to slow down with increasing solute concentration in the range of X_{acet} = 0−0.4 but becomes faster again for higher X_{acet}. For X_{acet} = 0.9 the anisotropy decay is even similar to the anisotropy decay of pure water (X_{acet} = 0). The composition of water−acetone mixtures, at which we find the slowest anisotropy decays of water molecules in Figure 7b (X_{acet} = 0.4), is somewhat different from the composition at which the self-diffusion coefficient of water molecules has a minimum, which occurs around X_{acet} = 0.2 as determined by NMR spin echo experiments.[10,34]

Since the anisotropy decays are obtained from an average over the bleaching signal, they represent the response of *all* types of water molecules in the sample, i.e., water molecules forming hydrogen bonds to other water molecules and water molecules forming hydrogen bonds to the S═O groups of DMSO and the C═O groups of acetone. As these different types of water molecules show different spectral responses, we

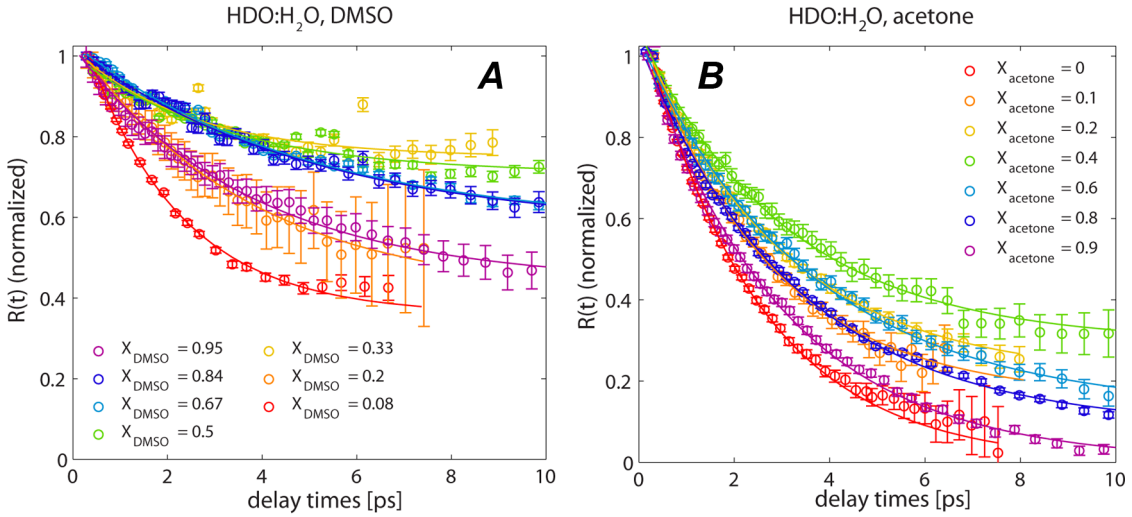

Figure 7. (A) Normalized anisotropy decay of the OD-stretch vibration of HDO molecules in aqueous DMSO solutions or X_{sol} = 0.08−0.95. The data have been averaged over a range of ∼70−90 cm^{-1} of the bleaching signal of the transient absorption spectra. (B) Normalized anisotropy decay of the OD-stretch vibration of HDO molecules in aqueous acetone solutions for X_{acet} = 0−0.9. The data have been averaged over a range of ∼100 cm^{-1} of the bleaching signal of the transient absorption spectra. The solid lines are serve as a guide to the eye.

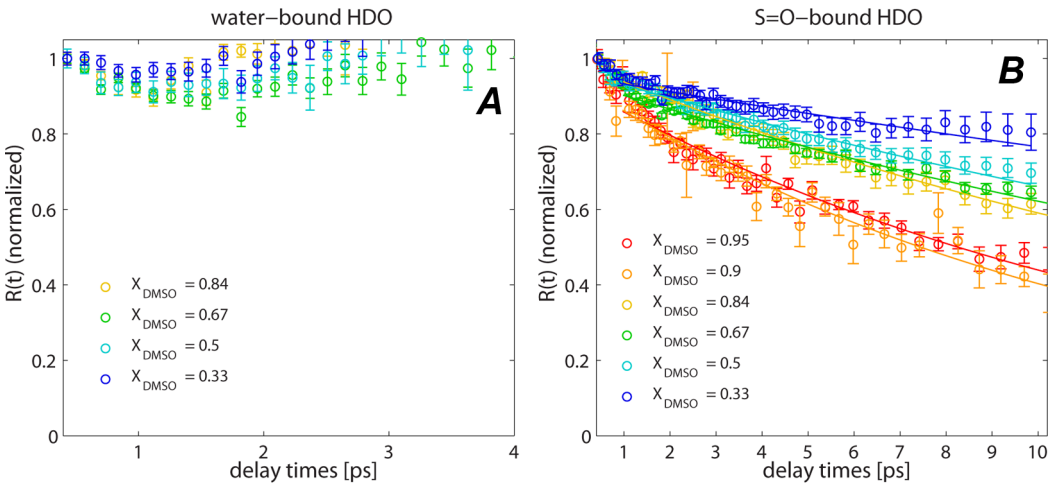

Figure 8. Anisotropy decays of water–DMSO solutions associated with the low- and high-frequency bands of which the amplitudes and T_1 time constants are shown in Figure 4. Panel A shows the decay of the anisotropy of the OD group of HDO molecules with their OD group hydrogen bonded to other water molecules for X_{DMSO} = 0.33–0.84, and panel B shows the decay for HDO molecules having their OD groups hydrogen bonded to the S=O group of DMSO. The anisotropy decays in this figure have been obtained by the decomposition of the polarization resolved transient absorption changes as outlined in the text. The solid lines in panel B are monoexponential fits.

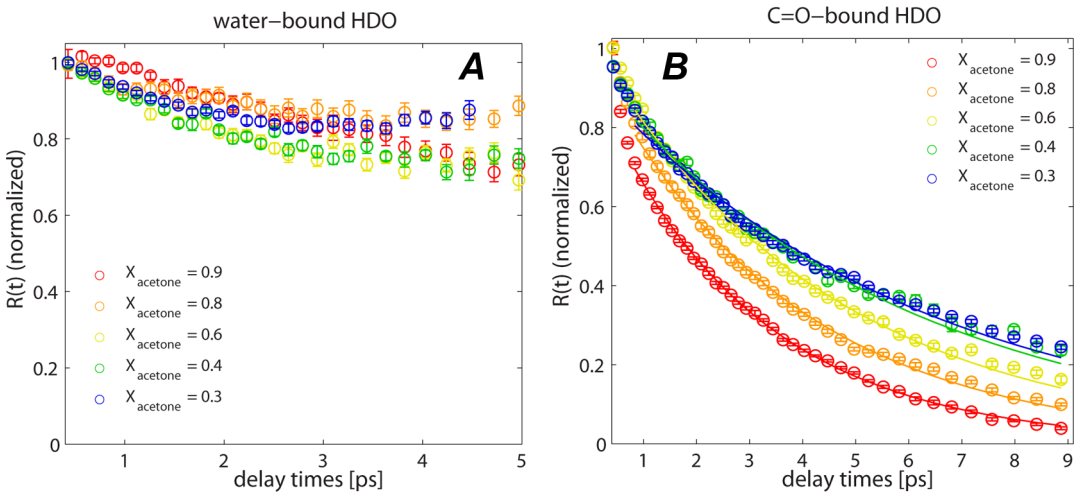

Figure 9. Anisotropy decays of water-acetone solutions at X_{acet} = 0.3–0.9. Panel A shows the decay of the anisotropy of the OD group of HDO molecules with their OD group hydrogen bonded to other water molecules, and panel B shows the corresponding decay for HDO molecules having their OD groups weakly hydrogen bonded to acetone. The anisotropy decays in this figure have been obtained by the decomposition of the polarization resolved transient absorption changes as outlined in the text. The solid lines in panel B are monoexponential fits.

can disentangle their contributions to the anisotropy dynamics. We use the spectral bands that we obtained from fitting the isotropic transient absorption changes $\Delta\alpha_{iso}(\omega,t)$ of water–DMSO and water–acetone mixtures with $X_{sol} \geq 0.3$, to perform a decomposition of the polarization-resolved data sets $\Delta\alpha_{\parallel}(\omega,t)$ and $\Delta\alpha_{\perp}(\omega,t)$. The resulting amplitudes of the two spectral bands in $\Delta\alpha_{\parallel}(\omega,t)$ and $\Delta\alpha_{\perp}(\omega,t)$ at different time delays are used to construct the anisotropy dynamics of the two bands. A detailed outline of the procedure and exemplary spectral bands for water-bound and S=O/C=O-bound HDO molecules are given in the Appendix.

For water–DMSO mixtures, the spectral response of the low-frequency band becomes quite small at high DMSO mole fractions, as seen in Figure 4a, which makes the determination of the anisotropy of the low-frequency band very noisy. For $X_{DMSO} \geq 0.9$ the transient absorption is dominated by the high-frequency band, and its anisotropy can still be well determined. In Figure 8 we present the anisotropy decay of the low-frequency water-bound band up to X_{DMSO} = 0.84 and the anisotropy decay of the high-frequency band up to X_{DMSO} = 0.95. The anisotropy $R_{WW}(t)$ of the low-frequency water-bound band (Figure 8a) is more or less constant, which means that the water-bound water molecules in water–DMSO mixtures show very little reorientation in the measured delay time interval. An analysis of the dynamics for delay times longer than 4 ps is obstructed by the comparably short vibrational lifetime of this type of water molecules ($T_1 \approx 2$ ps) and its relatively small amplitude (Figure 4a). The anisotropy $R_{WD}(t)$ of the high-frequency S=O group bound water molecules (Figure 8b) shows a slow exponential decay that becomes somewhat faster with increasing X_{DMSO}. The time constants of the reorientation are shown in Figure 10. The time constant decreases from 46 ± 14 ps at X_{DMSO} = 0.33 to 13 ± 2 ps at X_{DMSO} = 0.95.

The results of the decomposition analysis for the water–acetone mixtures are shown in Figure 9. In this figure we present the anisotropy decays $R_{WW}(t)$ of water-bound HDO

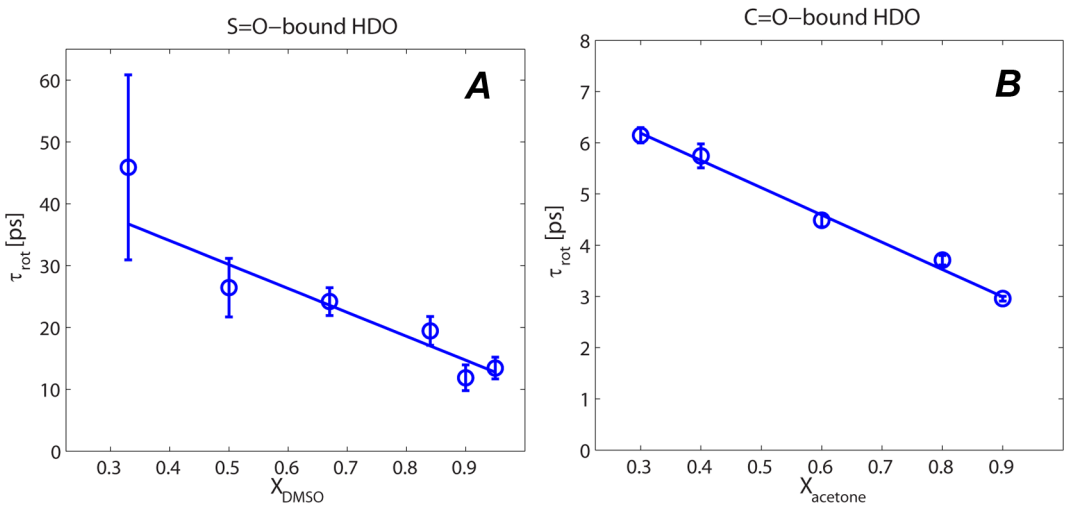

Figure 10. Time constants of the anisotropy decay of water molecules hydrogen bonded to the S═O group of DMSO as a function of X_{DMSO} (panel A) and the time constants of water molecules hydrogen bonded to the C═O group of acetone as a function of X_{acet} (panel B). The time constants are obtained from a single-exponential fit of the data shown in Figures 8b and 9b.

molecules (Figure 9a) and $R_{WA}(t)$, the anisotropy decay of HDO molecules that are hydrogen bonded to the C═O groups of acetone molecules (Figure 9b). $R_{WW}(t)$ shows only a partial decay to about 80−90% of the initial value within the first 4 ps. The results in Figure 9a show that water molecules that are hydrogen bonded to other water molecules are strongly impaired in their reorientation. It is likely that these water molecules are present in the form of small water clusters, which agrees with the fact that the vibrational lifetime of these water molecules is similar to that of neat water (Figure 4). The anisotropy $R_{WA}(t)$ of the C═O bound water shown in Figure 9b is much faster than that of the S═O bound water shown in Figure 8b. This difference can be explained from the fact that the hydrogen bond between water and the C═O group of acetone is much weaker than that between water and the S═O group of DMSO. Because of the weakness of the hydrogen bond to the C═O group, the barrier for reorientation is low, thus making the hydroxyl group highly mobile. This interpretation is supported by the observations that these water molecules absorb at high frequencies and have a long vibrational lifetime of $T_1 \approx 13$ ps. Both observations indicate that the hydrogen bond donated by the O−D groups of these HDO molecules is very weak. It is seen in Figure 9b that the decay of the anisotropy $R_{WA}(t)$ significantly accelerates with increasing acetone concentration. The time constants of the reorientation are shown in Figure 10 and decrease from 6.1 ± 0.2 ps at $X_{acet} = 0.3$ to 2.96 ± 0.05 ps at $X_{acet} = 0.9$.

For both water−DMSO and water−acetone mixtures the anisotropy decay of the water molecules that are hydrogen bonded to the solute becomes faster with increasing solute concentration (Figures 8b and 9b). This acceleration is likely due to the fact that the water molecules that donate a hydrogen bond to the S═O group of DMSO/C═O group of acetone will become less coordinated with other water molecules when the solute concentration increases. With increasing X_{DMSO}, the fraction of 1:1 water−DMSO complexes will increase over the fraction of 2:1 water−DMSO complexes. As a result, the water molecule that is hydrogen bonded to the S═O group will no longer accept a hydrogen bond from another water molecule, which increases its orientational mobility. It has been observed that upon addition of acetone to water the number of 4-fold coordinated water molecules, which is the prevalent species in pure water, is gradually reduced and that 3- and 2-fold coordinated water molecules become more prominent.[24,25] Hence, at high acetone content, water molecules that donate a hydrogen bond to the C═O group with one hydroxyl group no longer donate a hydrogen bond to a water molecule with their other hydroxyl group and no longer accept hydrogen bonds from other water molecules. As a result, the C═O bound water molecules become more mobile, leading to an acceleration of their reorientation.

The observed differences in vibrational relaxation and molecular reorientation dynamics of water molecules in water−DMSO and water−acetone mixtures likely find their origin in the different molecular geometries of the DMSO and acetone molecules. As mentioned in the Introduction, acetone adopts an essentially planar geometry, whereas the oxygen atom of a DMSO molecule lies outside the C−S−C plane. Additionally, the C−C and C═O bond lengths are considerably shorter than the C−S and S═O bonds in DMSO, respectively, making acetone an overall more compact molecule. It is conceivable that the specific molecular geometry of DMSO allows a water molecule to donate a hydrogen bond to the oxygen atom of the S═O group of DMSO with little steric hindrance from the methyl groups. In contrast, the methyl groups of acetone might pose a significant steric barrier for the formation of hydrogen bonds to the oxygen atom of the C═O group, due to the planar and overall more compact geometry of the acetone molecule.

4. CONCLUSIONS

We studied the vibrational energy relaxation and molecular reorientation dynamics of water molecules in water−DMSO and water−acetone mixtures with polarization-resolved femtosecond mid-infrared spectroscopy. For both water−DMSO and water−acetone mixtures we observe a slowing down of the vibrational relaxation dynamics of the water molecules with increasing solute fraction. For solute fractions $X_{sol} \geq 0.3$ the transient spectra show the presence of two components, corresponding to water molecules that are hydrogen bonded to other water molecules and water molecules that are hydrogen bonded to C═O or S═O groups. The vibrational relaxation

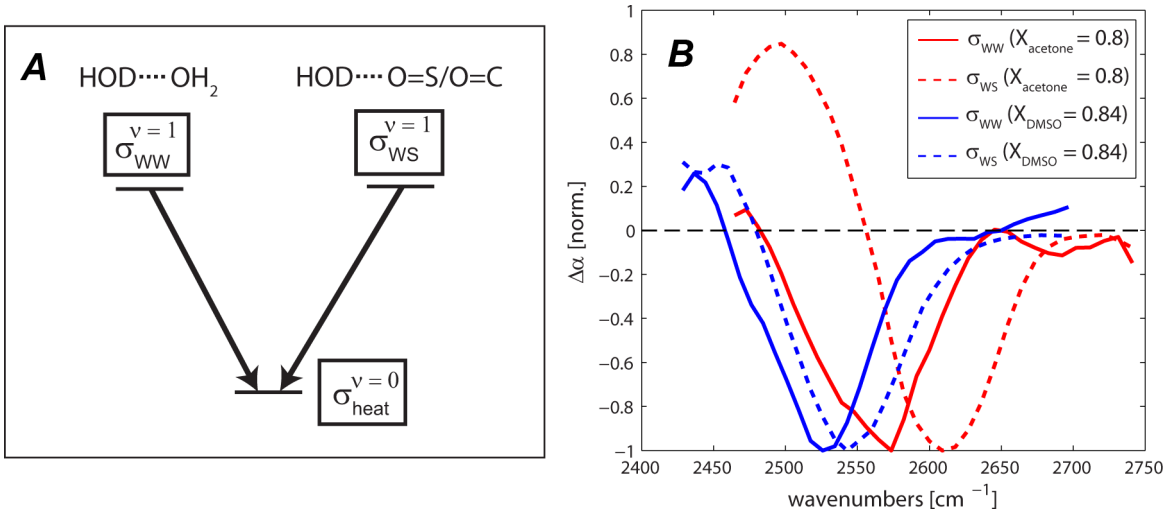

Figure 11. (A) Graphical representation of the model employed to describe the vibrational relaxation dynamics of the OD-stretch vibration of HDO molecules in water−DMSO and water−acetone mixtures. The excited states ($\nu = 1$) of water-bound (WW) and solute-bound (WS) HDO molecules decay to a common heated groundstate ($\nu = 0$). (B) Associated spectral signatures of the excited OD-stretch vibration of HDO molecules having their excited OD-group hydrogen bonded to other water molecules (lower frequency band) or the SO/CO moiety of DMSO/acetone. The spectra have been normalized to the maximum absolute value of the negative part of the spectra. The spectral separation between the two types of HDO species is about 20 cm^{-1} for DMSO−water and 50 cm^{-1} for acetone−water.

time constant T_1 of the C═O/S═O bound water molecules strongly increases with increasing solute fraction (Figure 4b), to 7.9 ps at X_{DMSO} = 0.95 and to 12.7 ps at X_{acet} = 0.9. This increase in vibrational lifetime can be explained from the decreased probability that the water molecule that is hydrogen bonded to S═O/C═O is involved in hydrogen bonds with other water molecules.

The water−DMSO and water−acetone mixtures show remarkable differences in the reorientation dynamics of the water molecules. At low solute fractions, we observe for both mixtures a fraction of water molecules that are strongly slowed down in their reorientation. We attribute this slow fraction to water molecules that hydrate the hydrophobic methyl groups. The fraction of slow water is much smaller for water−acetone than for water−DMSO at the same concentration. For water−acetone the slow fraction does not exceed ~20% of the total number of water molecules, and this plateau value is reached already at a solute concentration of X_{acet} = 0.05. This finding indicates that the acetone molecules form clusters already at low solute concentrations. With increasing solute fraction, the water−DMSO mixtures show a gradual transition from the effect of hydrophobic hydration to the effect of hydrogen bonding to the S═O group.

At high solute fractions, the water-bound water molecules in both water−acetone and water−DMSO mixtures show a very slow reorientation with a time constant ≫10 ps (Figures 9a and 8a). A difference between the two mixtures is that the amplitude of the water-bound water is much higher for water−acetone than for water−DMSO mixtures, which indicates that water forms nanoconfined water clusters in water−acetone mixtures. The water−acetone mixtures also contain water molecules that are weakly hydrogen bonded to the C═O group. These water molecules show a relatively fast reorientation with a time constant that decreases from 6.1 ± 0.2 ps at X_{acet} = 0.3 to 2.96 ± 0.05 ps at X_{acet} = 0.9 (Figure 9b). For water−DMSO mixtures the water molecules forming hydrogen bonds to the S═O group show a much slower reorientation (Figure 9b) with a time constant that decreases from 46 ± 14 ps at X_{DMSO} = 0.33 to 12 ± 2 ps at X_{DMSO} = 0.95. The large difference in reorientation time constant of the solute-bound water for DMSO and acetone is due to the fact that the hydrogen bond between water and the S═O group of DMSO is much stronger than the hydrogen bond between water and the C═O group of acetone.

Our observations support the notion of earlier studies that the structure of water−DMSO mixtures is largely determined by stable DMSO:water complexes for all mixture compositions, whereas the microscopic structure of water−acetone mixtures appears to be highly heterogeneous, showing nanoconfined acetone clusters at low acetone concentrations and nanoconfined water clusters at high acetone concentrations. This remarkable difference between water−DMSO and water−acetone mixtures is probably due to the difference in molecular structure between DMSO and acetone. The larger, bent DMSO molecule offers sufficient room for water molecules to form strong hydrogen bonds to the S═O group, while the more compact, planar acetone molecule does not provide sufficient room for a water molecule to form a strong hydrogen bond to the C═O group.

APPENDIX: FIT OF THE ISOTROPIC ABSORPTION CHANGES AND DECOMPOSITION OF THE ANISOTROPY DECAYS AT HIGH SOLUTE FRACTIONS

We use a model that is schematically represented in Figure 11A to fit the isotropic transient absorption changes $\Delta\alpha_{iso}(\omega,t)$. The spectral signatures of the excited OD-stretch vibration of water-bound (WW) and solute-bound (WS) HDO molecules for solute mole fractions of X_{DMSO} = 0.8 and X_{acet} = 0.84, respectively, are shown in Figure 11B.

When cast into matrix form, the set of ordinary differential equations associated with the vibrational relaxation model shown in Figure 11 read as follows:

$$\frac{\mathrm{d}}{\mathrm{d}t}\begin{pmatrix} N_{WW}(t) \\ N_{WS}(t) \\ N_{\mathrm{heat}}(t) \end{pmatrix} = \begin{pmatrix} -1/T_{WW} & 0 & 0 \\ 0 & -1/T_{WS} & 0 \\ 1/T_{WW} & 1/T_{WS} & 0 \end{pmatrix}\begin{pmatrix} N_{WW}(t) \\ N_{WS}(t) \\ N_{\mathrm{heat}}(t) \end{pmatrix} \tag{A1}$$

Numerical integration of the above equations yields the time-dependent population $N_i(t)$ of the three states included in the relaxation model. The best values for the vibrational lifetimes of water-bound HDO molecules T_{WW} and solute-bound HDO molecules T_{WS} are obtained by minimizing the target function

$$\chi^2(T_i) = \sum_k \left(\frac{\Delta\alpha_{\mathrm{iso}}(\omega, t_k) - \sum_i^n N_i(t_k; T_i)\sigma_i(\omega)}{\epsilon_{\mathrm{iso}}(\omega, t_k)} \right)^2 \tag{A2}$$

The frequency-dependent, spectral signature of the ith states $\sigma_i(\omega)$ are found by simultaneously finding the least-squares solution to the equation

$$\frac{\mathrm{d}}{\mathrm{d}\sigma_i(\omega_j)} \sum_j \left(\frac{\Delta\alpha_{\mathrm{iso}}(\omega_j, t) - \sum_i^n N_i(t; T_i)\sigma_i(\omega_j)}{\epsilon_{\mathrm{iso}}(\omega_j, t)} \right)^2 = 0 \tag{A3}$$

where i runs over all three states involved in the model of Figure 11A ($n = 3$).

Having obtained the spectral signatures of the excited states of water-bound and solute-bound HDO molecules, $\sigma_{WW}(\omega)$ and $\sigma_{WS}(\omega)$ are then used to disentangle the contribution from these distinct water species to the anisotropy decays in Figure 7A,B. The anisotropy decays associated with each of the two water species individually are found by performing a decomposition of the polarization-resolved transient absorption changes $\Delta\alpha_{\parallel}(\omega,t)$ and $\Delta\alpha_{\perp}(\omega,t)$. To that end, we write the transient absorption changes obtained under parallel and perpendicular polarization of pump and probe pulses as

$$\Delta\alpha_{\parallel}(\omega, t) = \sum_{i=1}^{n} (1 + 2R_i(t))N_i(t)\sigma_i(\omega) = \sum_{i=1}^{n} N_{i,\parallel}(t)\sigma_i(\omega) \tag{A4a}$$

$$\Delta\alpha_{\perp}(\omega, t) = \sum_{i=1}^{n} (1 - R_i(t))N_i(t)\sigma_i(\omega) = \sum_{i=1}^{n} N_{i,\perp}(t)\sigma_i(\omega) \tag{A4b}$$

where $R_i(t)$ denotes the anisotropy of a given species i of water molecules, which is assumed to have no frequency dependence, and the sum runs over all water species contributing to the transient absorption changes. Since the heated ground state ($i = 3$) represents a thermal difference spectrum, it is assumed to be isotropic and not to contribute to the anisotropy decay. Therefore, the signal contribution of the heated ground state is subtracted and the decomposition is performed with the two excited states only ($n = 2$ in eq A4). The decomposition of the polarization resolved data sets $\Delta\alpha_{\parallel}(\omega,t)$ and $\Delta\alpha_{\perp}(\omega,t)$ with the previously obtained $\sigma_{WW}(\omega)$, $\sigma_{WS}(\omega)$ is based on finding the least-squares solution to the equation

$$\frac{\mathrm{d}}{\mathrm{d}N_{i,\parallel}(t_k)} \sum_k \left(\frac{\Delta\alpha_{\parallel}(\omega, t_k) - \sum_i N_{i,\parallel}(t_k)\sigma_i(\omega)}{\epsilon_{\parallel}(\omega, t_k)} \right)^2 = 0 \tag{A5}$$

The same procedure is performed for $\Delta\alpha_{\perp}$. Having obtained $N_{i,\parallel}(t)$ and $N_{i,\perp}(t)$, it is possible to extract the anisotropy decay that reflects purely the reorientation dynamics of the ith water species:

$$R_i(t) = \frac{N_{i,\parallel}(t) - N_{i,\perp}(t)}{N_{i,\parallel}(t) + 2N_{i,\perp}(t)} \tag{A6}$$

The results of this analysis are shown in Figures 8 and 9.

AUTHOR INFORMATION

Corresponding Author

*E-mail: lotze@amolf.nl (S.L.).

Notes

The authors declare no competing financial interest.

ACKNOWLEDGMENTS

This work is part of the research program of the "Stichting voor Fundamenteel Onderzoek der Materie (FOM)", which is financially supported by the "Nederlandse organisatie voor Wetenschappelijk Onderzoek (NWO)".

REFERENCES

(1) Riddick, J.; Bunger, W. B.; Sakano, T. K. *Organic Solvents: Physical Properties and Methods of Purification*; John Wiley and Sons: New York, 1986.

(2) NIST Chemistry WebBook.

(3) Cowie, J. M. G.; Toporowski, P. M. Association in the Binary Liquid System Dimethyl Sulfoxide - Water. *Can. J. Chem.* **1961**, *39*, 2240−2243.

(4) Hanson, D. O.; Van Winkle, M. Relation of Binary Heats of Mixing and Distribution of Ketone between Phases in Some Ketone-Water-Solvent Ternaries. *J. Chem. Eng. Data* **1960**, *5*, 30−34.

(5) Schichman, S. A.; Amey, R. L. Viscosity and Local Liquid Structure in Dimethyl Sulfoxide-Water Mixtures. *J. Phys. Chem.* **1971**, *75*, 98−102.

(6) Padova, J. Ion-Solvent Interaction in Mixed Solvents. II. The Viscosity of Electrolytes in Mixed Solvents. *J. Chem. Phys.* **1963**, *38*, 2635−2640.

(7) Kaatze, U.; Pottel, R.; Schaefer, M. Dielectric Spectrum of Dimethyl Sulfoxide/Water Mixtures as a Function of Composition. *J. Phys. Chem.* **1989**, *93*, 5623−5627.

(8) Kumbharkhane, A.; Helambe, S.; Lokhande, M.; Doraiswamy, S.; Mehrotra, S. Structural Study of Aqueous Solutions of Tetrahydrofuran and Acetone Mixtures Using Dielectric Relaxation Technique. *Pramana* **1996**, *46*, 91−98.

(9) Packer, K. J.; Tomlinson, D. J. Nuclear Spin Relaxation and Self-diffusion in the Binary System, Dimethylsulfoxide (DMSO) + Water. *Trans. Faraday Soc.* **1971**, *67*, 1302−1314.

(10) McCall, D. W.; Douglass, D. C. Diffusion in Binary Solutions. *J. Phys. Chem.* **1967**, *71*, 987−997.

(11) Lovelock, J. E.; Bishop, M. W. H. Prevention of Freezing Damage to Living Cells by Dimethyl Sulfoxide. *Nature* **1959**, *183*, 1394−1395.

(12) Bickis, I.; Kazaks, K.; Finn, J.; Henderson, I. Permeation Kinetics of Glycerol and Dimethyl Sulfoxide in Novikoff Hepatoma Ascites Cells. *Cryobiology* **1967**, *4*, 1−10.

(13) Ashwood-Smith, M. J. Preservation of Mouse Bone Marrow at −79 °C. with Dimethyl Sulfoxide. *Nature* **1961**, *190*, 1204−1205.

(14) Pegg, D. Freezing of Bone Marrow for Clinical Use. *Cryobiology* **1964**, *1*, 64−71.

(15) Ashwood-Smith, M. J. Radioprotective and Cryoprotective Properties of Dimethyl Sulfoxide in Cellular Systems. *Ann. N. Y. Acad. Sci.* **1967**, *141*, 45−62.

(16) Vicente, J.; Garciaa-Ximenez, F. Osmotic and Cryoprotective Effects of a Mixture of DMSO and Ethylene Glycol on Rabbit Morulae. *Theriogenology* **1994**, *42*, 1205−1215.

(17) Hanslick, J. L.; Lau, K.; Noguchi, K. K.; Olney, J. W.; Zorumski, C. F.; Mennerick, S.; Farber, N. B. Dimethyl sulfoxide (DMSO)

744 Produces Widespread Apoptosis in the Developing Central Nervous
745 System. *Neurobiol. Dis.* **2009**, *34*, 1−10.
746 (18) Borin, I. A.; Skaf, M. S. Molecular Association between Water
747 and Dimethyl Sulfoxide in Solution: A Molecular Dynamics
748 Simulation Study. *J. Chem. Phys.* **1999**, *110*, 6412−6420.
749 (19) Luzar, A.; Chandler, D. Structure and Hydrogen Bond
750 Dynamics of Water-Dimethyl Sulfoxide Mixtures by Computer
751 Simulations. *J. Chem. Phys.* **1993**, *98*, 8160−8173.
752 (20) Vaisman, I. I.; Berkowitz, M. L. Local Structural Order and
753 Molecular Associations in Water-DMSO Mixtures. Molecular
754 Dynamics Study. *J. Am. Chem. Soc.* **1992**, *114*, 7889−7896.
755 (21) Soper, A. K.; Luzar, A. A Neutron Diffraction Study of Dimethyl
756 Sulfoxide-Water Mixtures. *J. Chem. Phys.* **1992**, *97*, 1320−1331.
757 (22) Kirchner, B.; Reiher, M. The Secret of Dimethyl Sulfoxide-
758 Water Mixtures. A Quantum Chemical Study of 1DMSO-n Water
759 Clusters. *J. Am. Chem. Soc.* **2002**, *124*, 6206−6215.
760 (23) Wong, D. B.; Sokolowsky, K. P.; El-Barghouthi, M. I.; Fenn, E.
761 E.; Giammanco, C. H.; Sturlaugson, A. L.; Fayer, M. D. Water
762 Dynamics in Water/DMSO Binary Mixtures. *J. Phys. Chem. B* **2012**,
763 *116*, 5479−5490.
764 (24) Ferrario, M.; Haughney, M.; McDonald, I. R.; Klein, M. L.
765 Molecular-Dynamics Simulation of Aqueous Mixtures: Methanol,
766 Acetone, and Ammonia. *J. Chem. Phys.* **1990**, *93*, 5156−5166.
767 (25) Venables, D. S.; Schmuttenmaer, C. A. Spectroscopy and
768 Dynamics of Mixtures of Water with Acetone, Acetonitrile, and
769 Methanol. *J. Chem. Phys.* **2000**, *113*, 11222−11236.
770 (26) McLain, S. E.; Soper, A. K.; Luzar, A. Investigations on the
771 Structure of Dimethyl Sulfoxide and Acetone in Aqueous Solution. *J.*
772 *Chem. Phys.* **2007**, *127*.
773 (27) Max, J.-J.; Chapados, C. Infrared Spectroscopy of Acetone-
774 Water Liquid Mixtures. I. Factor Analysis. *J. Chem. Phys.* **2003**, *119*,
775 5632−5643.
776 (28) Max, J.-J.; Chapados, C. Infrared Spectroscopy of Acetone-
777 Water Liquid Mixtures. II. Molecular Model. *J. Chem. Phys.* **2004**, *120*,
778 6625−6641.
779 (29) Steinel, T.; Asbury, J. B.; Zheng, J.; Fayer, M. D. Watching
780 Hydrogen Bonds Break: A Transient Absorption Study of Water. *J.*
781 *Phys. Chem. A* **2004**, *108*, 10957−10964.
782 (30) Rezus, Y. L. A.; Bakker, H. J. On the Orientational Relaxation of
783 HDO in Liquid Water. *J. Chem. Phys.* **2005**, *123*.
784 (31) Rezus, Y. L. A.; Bakker, H. J. Observation of Immobilized Water
785 Molecules around Hydrophobic Groups. *Phys. Rev. Lett.* **2007**, *99*,
786 148301.
787 (32) Rezus, Y.; Bakker, H. Femtosecond Spectroscopic Study of the
788 Solvation of Amphiphilic Molecules by Water. *Chem. Phys.* **2008**, *350*,
789 87−93.
790 (33) Benedetti, A.; Cilense, M.; Vollet, D.; Montone, R.
791 Thermodynamic properties of liquid mixtures. III. Acetone water.
792 *Thermochim. Acta* **1993**, *66*, 219−223.
793 (34) Von Goldammer, E.; Hertz, H. G. Molecular Motion and
794 Structure of Aqueous Mixtures with Nonelectrolytes As Studied by
795 Nuclear Magnetic Relaxation Methods. *J. Phys. Chem.* **1970**, *74*, 3734−
796 3755.